

INP-BASED DEVICES AND CIRCUITS FOR HIGH PERFORMANCE MICROWAVE/MILLIMETER WAVE APPLICATIONS

Paul T. Greiling

Hughes Research Laboratories
3011 Malibu Canyon Road
Malibu, CA 90265

ABSTRACT

InP-based (AlInAs/GaInAs) high electron mobility transistors (HEMTs) and heterojunction bipolar transistors (HBTs) have demonstrated a substantial performance improvement over GaAs-based devices. HEMTs with extrinsic f_T 's over 300 GHz, f_{max} 's over 400 GHz, and amplifiers with extremely low noise figures and high associated gain ($NF < 0.7$ dB, $G_{assoc} > 12$ dB at 12 GHz and $NF < 1.8$ dB, $G_{assoc} > 6$ dB at 60 GHz) have been achieved. HBTs have exhibited f_T 's exceeding 130 GHz with f_{max} 's of 80 GHz. Digital and analog ICs have shown state-of-the-art performance: a 36 GHz divide by 4, a 9 GHz 8/9 dual modulus divider, a 16 GHz active mixer, and a dc coupled feedback amplifier with 33 GHz bandwidth. The status of these device technologies for high performance microwave and millimeter-wave applications is discussed.

INTRODUCTION

Indium phosphide (InP)-based high electron mobility transistor (HEMT) and heterojunction bipolar transistor (HBT) technologies offer a significant performance advantage over gallium arsenide (GaAs)-based HEMTs and HBTs for microelectronic and optoelectronic applications. The higher performance of InP-based devices is due in part to the superior electronic transport properties, thermal conductivity and optical characteristics of the material system; however, the status of InP technology is generally behind that of GaAs technology, which in turn is immature compared with that of silicon (Si) technology. The commercial incentives for industrial development of these high performance technologies have been low, with the exception of the applications to photoemitters and photodetectors for fiber optic (FO) communications. The technology has been driven mainly by military requirements; however, with the emergence of direct broadcast systems (DBS), cellular telephone, and automotive collision avoidance systems, potential commercial opportunities are arising.

Future military as well as commercial communication and radar systems will require high-performance microwave and millimeter-wave devices and ICs. One of the most important applications is for low-noise amplifiers for receiver front ends and power amplifiers for phased array radars. Lower noise figure devices reduce requirements in antenna size, transmitter power and receiver assembly cost. For low noise and millimeter-wave power requirements, the HEMT is the obvious choice; however, for digital, linear, analog, A/D conversion applications, the HBT appears to have the most advantages. Only in the area of microwave power (<20 GHz) is there a question as to the best device for the application. Higher speed HBT analog and digital circuits will allow for wider bandwidths, higher data rates and lower complexity ICs.

HEMT PERFORMANCE

Recent advances in material growth and fabrication process technology have made possible the realization of ultrahigh frequency HEMTs in the AlInAs/GaInAs material system. In the last four years, through improvements in materials and shrinking of gatelength, the high frequency performance, the short circuit unity gain frequency, of state-of-the-art HEMTs has been increased at an astounding rate, as shown in Figure 1.

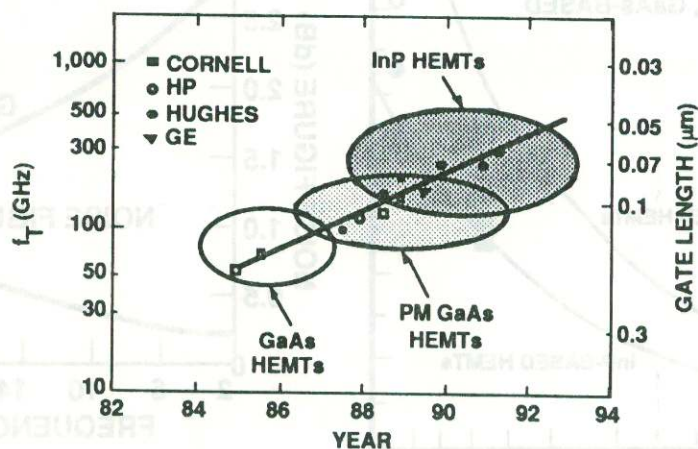


Figure 1. Published unity current-gain frequency and corresponding gatelength as a function of time for GaAs-based and InP-based HEMTs.

The unique properties of the InP-based AlInAs/GaInAs material system have clearly established this system as the leading candidate for millimeter-wave (MMW) ultra-low-noise applications. The cross section of the Field Effect Transistor (FET) is shown in Figure 2, illustrating the layer design for the four most common III-V semiconductor material systems. Compared to its closest competing technology—the GaAs-based pseudomorphic AlGaAs/Ga_{1-x}In_xAs material system, where $x < 0.3$ —the AlInAs/GaInAs system exhibits a 25 percent higher electron sheet density (3.5 versus $2.8 \times 10^{12} \text{ cm}^{-2}$) and a 60 percent higher room-temperature mobility ($10,000$ versus $7,000 \text{ cm}^2/\text{Vs}$), which results in significant advantages for InP-based HEMTs by reducing device parasitics and increasing the transconductances. The electron peak velocity is $2.7 \times 10^7 \text{ cm/s}$ compared to $2.1 \times 10^7 \text{ cm/s}$, and the Γ -L valley energy difference is 0.55 eV vs. 0.31 eV for GaInAs vs. GaAs. These differences result in a much shorter transit time under the gate and a higher overshoot velocity. These factors enhance noise figure, reduce the saturation voltage (knee voltage) and increase the high frequency operation.

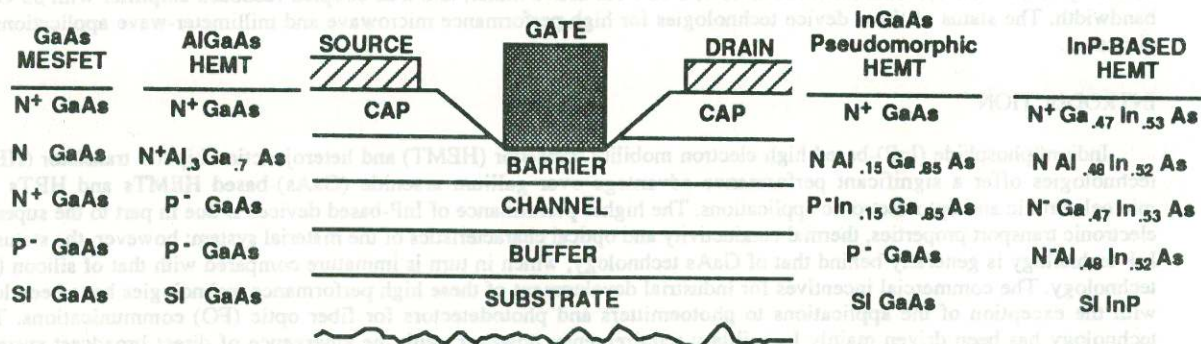


Figure 2. III-V compound semiconductor FET structures.

When all factors have been taken into account, the InP-based HEMT exhibits noise figures (NF) significantly lower than that of GaAs-based HEMTs, especially at millimeter-wave frequencies as shown in Figure 3.

Ultralow noise operation has been achieved for the AlInAs/GaInAs HEMT over a wide range of frequencies. For a $0.15 \times 300 \mu\text{m}$ gate HEMT, the measured on-wafer S- and noise parameters predict a noise figure as a function of frequency from 2 to 26 GHz, as plotted in Figure 4. Amplifiers incorporating these HEMTs have produced noise figures in the range of 0.65 to 0.7 dB with 13 dB gain.

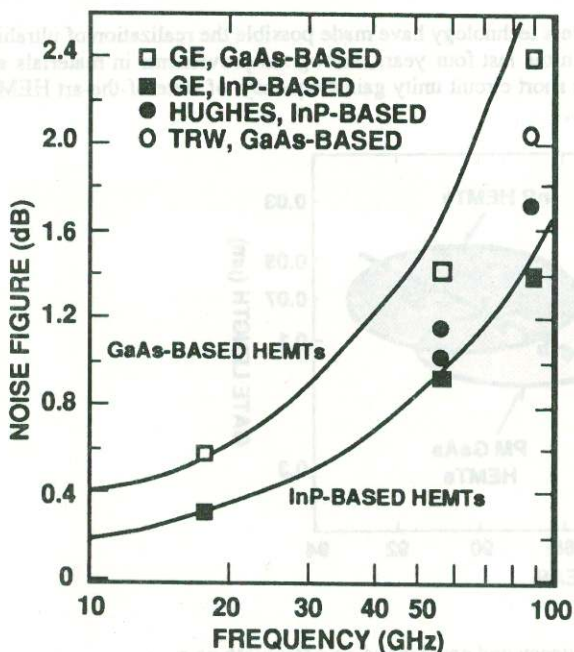


Figure 3. Published minimum noise figures as a function of time for GaAs-based and InP-based HEMTs.

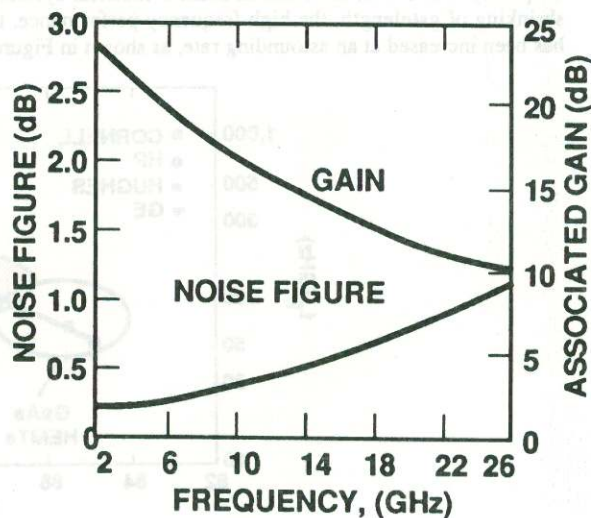


Figure 4. S- through Ku-band low noise HEMT performance.

We have performed extensive work on the device design, metallurgy and evaluation to develop a reliable AlInAs/GaInAs HEMT. Through proper ohmic contact, Schottky gate/barrier and active channel designs, we have demonstrated MTTF of greater than 10^8 h for 45°C operation. Amplifiers have less than 0.3 dB noise figure degradation and less than 0.8 dB gain increase after 1000 h at 150°C . The device performance has also been shown to be reproducible from wafer to wafer.

With the recent development of a InP via process, MMICs are being demonstrated. A 12 GHz low noise, single-stage MMIC amplifier exhibited a 0.78 dB noise figure with 15 dB gain. A three stage S-band LNA shown in Figure 5(a) demonstrated 0.5 dB noise figure with 36 dB gain as plotted in Figure 5(b).

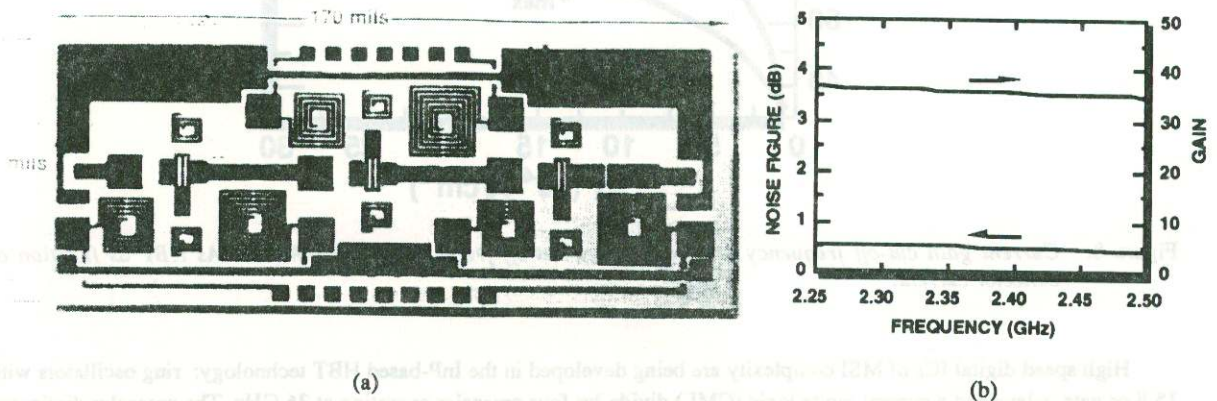


Figure 5. A 3 stage low-noise MMIC.

HBT PERFORMANCE

The advantages of the InP-based HBT are: (1) the large conduction band discontinuity between the emitter and the base, which launches the electrons at much higher velocities into the base coupled with the higher electron mobility in the heavily doped base, (2) the higher electron velocity in the collector due to higher peak velocity and large Γ -L valley energy difference, (3) the smaller band gap resulting in smaller base-emitter voltage drop and permitting lower operating voltages and power dissipation, (4) the lower surface recombination velocity improves scaling of current gain for small emitter sizes and low current densities and also leads to low $1/f$ noise, and (5) the thermal conductivity of InP is approximately 50% higher than GaAs; thereby allowing for higher power dissipation. The cross section of the InP-based HBT structure is shown in Figure 6. A comparison of the Gummel plots for InP-based and GaAs-based HBTs, shown in Figure 7(a) and 7(b), demonstrates several of these advantages. First, due to the high surface recombination velocity in AlGaAs, the HBT does not have gain (i.e., $I_C/I_B < 1$ at low current levels). Secondly, due to the lower band gap of GaInAs, the turn-on voltage of the InP-based HBT is similar to a Si bipolar. Thus, the InP-based HBT is a "drop in" for the Si bipolar, but with approximately five times the performance. The figure of merit for our HBT devices (f_T and f_{max}) is shown in Figure 8, exhibiting an f_T of 130 GHz and an f_{max} of 80 GHz. Though these values are comparable with the AlGaAs HBT, the previously mentioned advantages favor the InP-based HBT for high performance ICs.

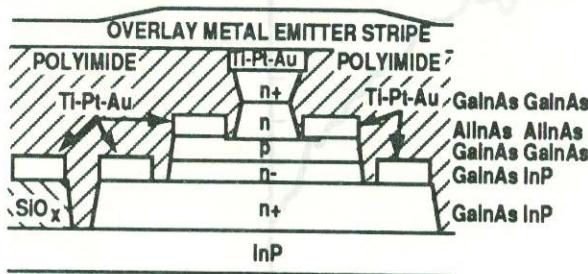


Figure 6. AlInAs/GaInAs HBT cross section.

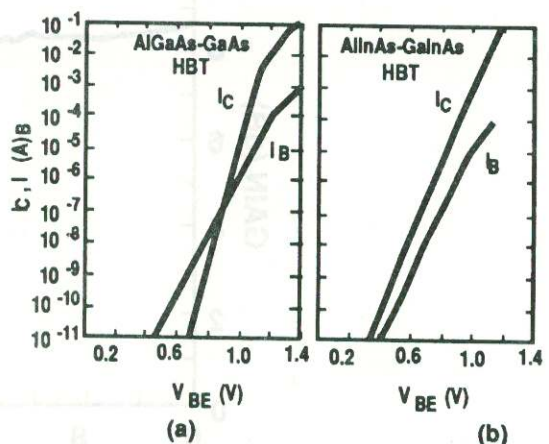


Figure 7. AlGaAs/GaAs HBT and AlInAs/GaInAs HBT Gummel plots.

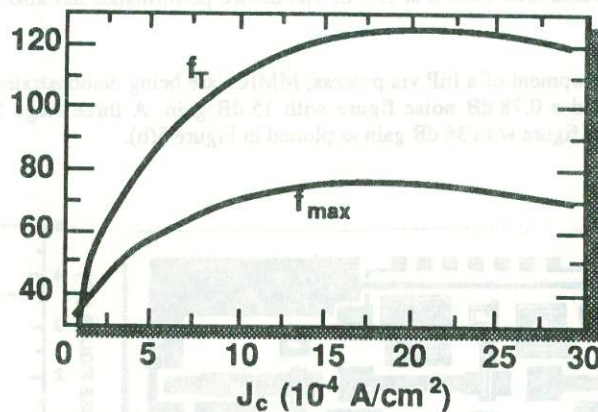


Figure 8. Current gain cut-off frequency and power gain cut-off frequency for AlInAs/GaInAs HBT as function of collector current.

High speed digital ICs of MSI complexity are being developed in the InP-based HBT technology: ring oscillators with 15.8 ps gate delays and a current mode logic (CML) divide-by-four prescaler operating at 36 GHz. The prescaler dissipated 500 mW for the entire chip including two flip-flops, a level shift stage and an output buffer amplifier to drive 50 Ω at 36 GHz. Larger complexity digital circuits have also been demonstrated such as a dual modules divider operating at 9 GHz.

In addition, a dc coupled feedback amplifier has been fabricated. Compared to matched amplifiers (MMICs), feedback amplifiers have a smaller bandwidth for a given f_{max} ; however, they occupy much smaller die area and have well-controlled characteristics determined by the feedback elements. This results in lower cost and higher levels of integration. In Si bipolar technology, feedback amplifiers have a broad range of applications below 4 GHz where they are limited by their transistor f_{max} . With the much higher f_{max} attainable in the InP-based HBT technology, these applications can now be extended to millimeter-wave frequencies. An active-bias cascode feedback amplifier was simulated and fabricated in the AlInAs/GaInAs HBT technology. The measured S_{21} exhibited a low frequency gain of 8.6 dB and a bandwidth at the -3 dB point of 33 GHz (Figure 9). Reverse isolation was greater than -14 dB at all frequencies. The output power is ~5 dBm at the 1 dB gain compression point.

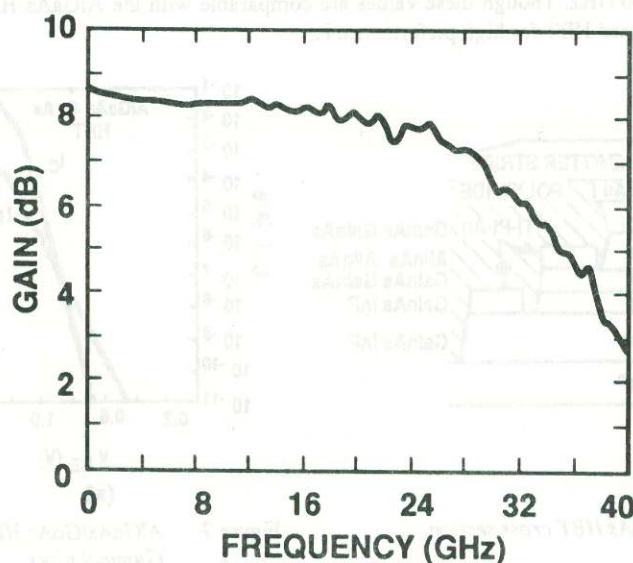


Figure 9. Gain vs. frequency for InP-based HBT feedback amplifier.

The frequency translation function in most microwave systems is performed by diode mixers. Diode mixers are simple passive circuits capable of operating at very high frequencies. Unfortunately, these mixers exhibit a conversion loss of 3.9 dB, or more typically 6 to 8 dB. Figure 10 shows a micrograph of the InP double-balanced active mixer. Inputs and outputs have been brought out differentially for maximum flexibility, but the chip can be used in a single-ended format. The mixer requires +10 and -5.2 V power supplies and dissipates 1 W. The die is 0.188×1.135 mm. The mixer is designed to have a conversion gain of +0 dB for a single-ended input and differential outputs. With both a single-ended input and output, the mixer has 6 dB conversion loss and, as expected, 3 dB of gain with differential inputs and outputs. Figure 11 shows a -3 dB bandwidth of 16 GHz for single-ended I/O conversion gain.

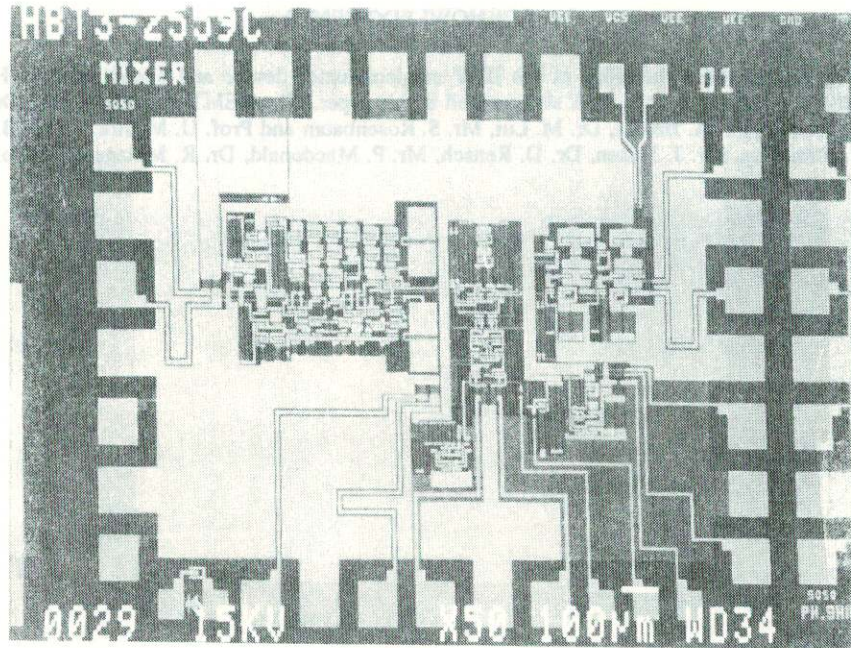


Figure 10. Micrograph of InP MMIC mixer.

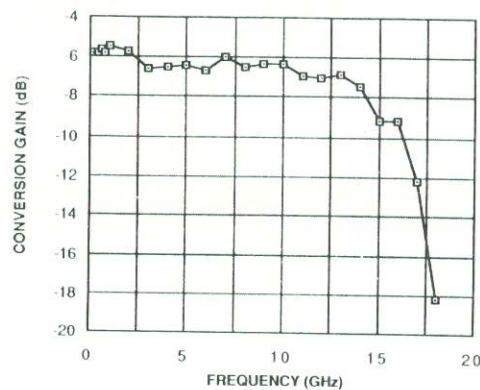


Figure 11. Conversion gain versus frequency for single-ended input and output (Swept LO/RF frequencies, $f_{RF} = f_{LO}$ -100 MHz, $P_{RF} = -20$ dBm, $P_{LO} = 0$ dBm).

The frequency response function of most microwave systems is performed by the use of the noise figure. The noise figure is a measure of the degradation of the signal-to-noise ratio (SNR) which occurs when a signal is passed through a device. The noise figure is defined as the ratio of the SNR at the input of the device to the SNR at the output of the device. The noise figure is a measure of the degradation of the SNR which occurs when a signal is passed through a device. The noise figure is a measure of the degradation of the SNR which occurs when a signal is passed through a device.

6.0 CONCLUSION

InP-based HEMT and HBT technologies have demonstrated the lowest microwave/millimeter-wave noise figure amplifiers, the highest speed digital ICs and the broadest bandwidth analog ICs. Combining this high performance InP-based device technology in optoelectronic system applications will extend integrated system performance into the millimeter-wave frequency range.

7.0 ACKNOWLEDGMENTS

I would like to acknowledge the work of the III-V semiconductor device and circuit team at Hughes Research Laboratories, which is responsible for the work summarized in this paper. The HEMT team consists of Dr. L. Nguyen, Dr. L. Larson, Dr. M. Delaney, Dr. A. Brown, Dr. M. Lui, Mr. S. Rosenbaum and Prof. U. Mishra of UCSB. The HBT team consists of Dr. W. Stanchina, Mr. J. Jensen, Dr. D. Rensch, Mr. P. Macdonald, Dr. R. Metzger and Prof. M. Rodwell of UCSB.

